

# Material Property Estimation for Direct Detection of DNAPL using Integrated Ground-Penetrating Radar Velocity, Imaging and Attribute Analysis

John H. Bradford, Scott B. Smithson, and W. Stephen Holbrook  
Geology and Geophysics, University of Wyoming

## ABSTRACT

We will test and develop a suite of methodologies for direct detection of pooled and residual DNAPLs from surface ground-penetrating radar (GPR) data. This is a new, quantitative approach to the analysis of GPR data in which we determine material properties remotely by quantifying signal characteristics such as propagation velocity and waveform attributes including amplitude, frequency content, and phase. With careful consideration of the physics governing electromagnetic (EM) wave propagation, these properties can be extracted from GPR data to characterize variations in electric properties. Many DNAPLs, including chlorinated solvents, have much lower dielectric permittivity and conductivity than water. A contrast in electric properties is induced when DNAPL displaces water in the sediment column resulting in an anomalous GPR attribute signature. The attribute signature can be exploited for remote DNAPL detection.

In our approach, we focus on three aspects of reflected wave behavior - propagation velocity, frequency dependent attenuation, and amplitude variation with offset. Velocity analysis provides a direct estimate of dielectric permittivity, attenuation analysis is used to identify variations in conductivity, and AVO behavior is used to quantify the dielectric permittivity ratio at a reflecting boundary. Attribute analysis is integrated with sophisticated signal processing methodologies, not commonly applied in GPR investigation, which dramatically improve image resolution and spatial accuracy. We have completed much of the preliminary work to include theoretical development, numerical and physical modeling studies, and initial development of attenuation and AVO attribute extraction algorithms.

The next step in development of these methods is rigorous field testing under a variety of hydrogeologic conditions. To this end, the focus of our proposed work is field investigation. We have identified a number of sites suitable for controlled GPR investigation including the Savannah River, SC, and Hanford, WA, sites, and four facilities designated as National Environmental Technology Test Sites (Dover AFB, DE; McClellan AFB, CA; Port Hueneme, CA; Wurtsmith AFB, CA). We propose to conduct a series of controlled and uncontrolled GPR experiments over known NAPL source areas at these sites. An integral part of data analysis will be continued development of attribute extraction algorithms. These algorithms will include methods for automated attribute extraction and material property estimation based on the physics of EM wave propagation.

Previous GPR NAPL detection studies have relied on minimal data processing and qualitative interpretation of subsurface profiles. Our approach combines sophisticated processing methodology with quantitative attribute analysis and material property estimation. The proposed research will lead to more efficient processing, reliable, accurate interpretations, and detection of subtle variations that are difficult or impossible to identify through qualitative interpretation alone. Implementation of these methodologies will be a significant advance in GPR research and in meeting DOE's need for reliable in-situ characterization of DNAPL contamination.



Figure 1: Locations of proposed GPR field studies. To date, data have been acquired at the Savannah River and Hill Air Force Base sites.

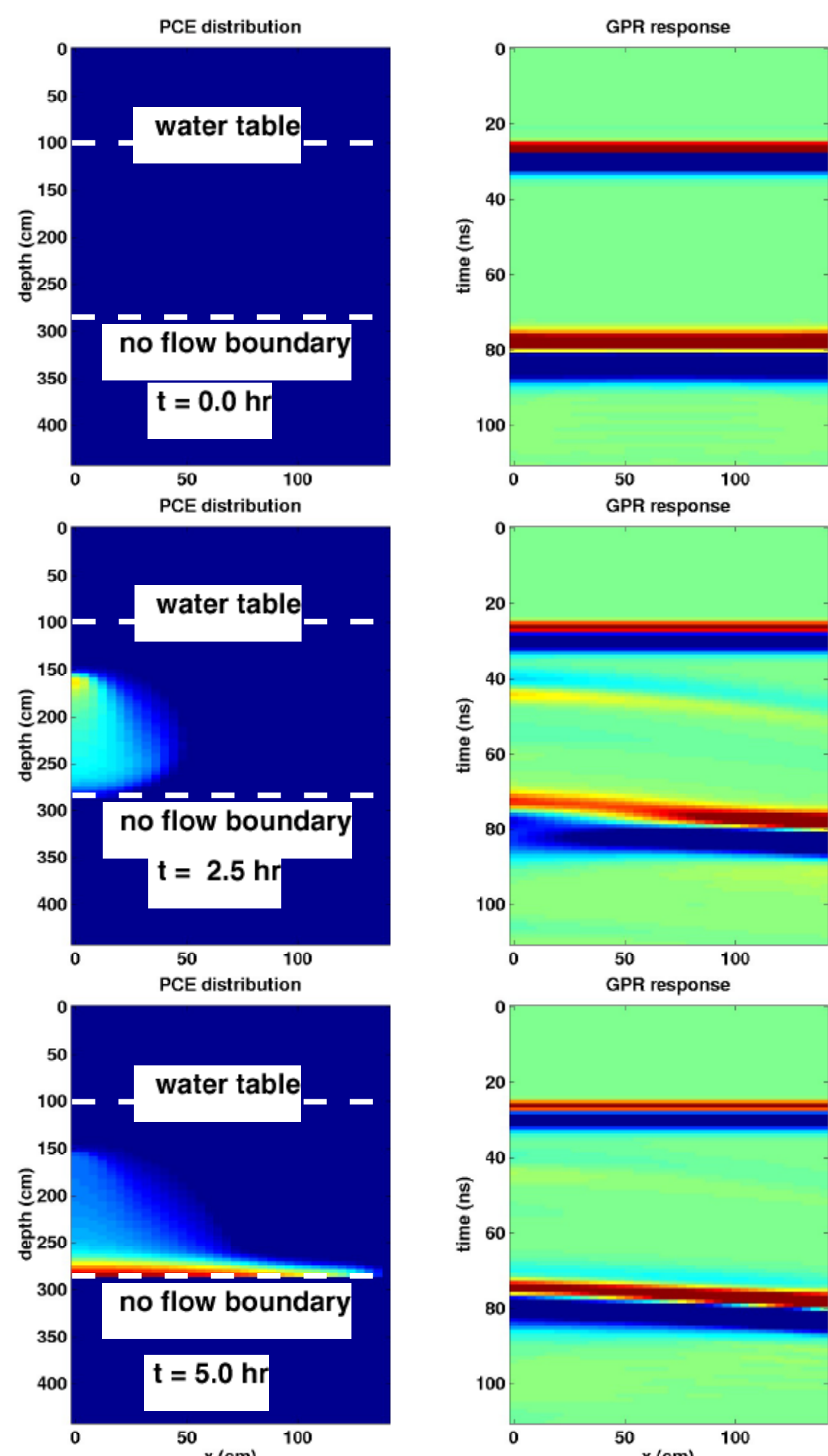


Figure 2: Two-phase flow simulation and GPR response at 100 MHz for a 50 l PCE injection in the saturated zone of a sandy aquifer. The maximum DNAPL concentration at 2.5 hrs is 39%, the maximum at 5 hrs is 59%. The injection was complete at 4.2 hrs.

## GPR AVO Analysis

Amplitude versus offset (AVO) analysis is a multi-offset attribute analysis technique used to study changes in reflection amplitude with increasing angles of incidence (Castagna, 1993). For EM wave propagation, the AVO response depends strongly on the contrast of electric permittivity and conductivity between the incident and reflecting medium (Lehmann, 1996).

There is also a strong dependence on the polarization of the electric field. In GPR studies, the polarization of the electric field is controlled by orientation of the transmitting and receiving antennas. We refer specifically to two antenna orientations as defined in Figure 3. Transverse polarization is the mode most commonly employed in GPR surveys, for both bi-static and multi-offset modes, but the AVO response for transverse and parallel polarization are dramatically different. Bradford (in revision), and Bradford et al. (in revision) demonstrated that parallel polarization holds the greatest potential for identifying contaminant saturated zones. The remainder of this discussion is focused on parallel polarization.

Figure 4 shows a hypothetical model for an unconfined aquifer contaminated with LNAPL and DNAPL. Material properties for the model were taken from data published by Powers and Olhoeft for moist sand, water saturated sand, gasoline saturated sand, PCE saturated sand, and clay. We calculated the parallel polarized AVO response for 6 cases (Figure 4) that would be encountered in a GPR survey at this site. It is clear that the response of the reflected wave varies significantly, depending on the type of fluid filling the pore space. The most striking feature of the reflection coefficient curves is the presence of Brewster's angle ( $\theta_B$ ). At this angle, the reflected wave is polarized by the out-of-phase component of the incident wave and no energy is reflected. We find that  $\theta_B$  occurs at much smaller angles of incidence, and the AVO gradient is significantly larger for reflections from the top of the NAPL saturated zones. In fact, the parallel polarized GPR AVO response is more substantial than is typically observed in seismic AVO studies for hydrocarbon exploration, and we expect similar or better success rates in GPR studies.

## Physical Model Data Analysis using AVO

As an initial feasibility study, Bradford et al. (in revision) constructed a physical experiment in the GPR test pit at the Houston Advanced Research Center. We buried two plastic containers, one containing water saturated sand (WC), and the other containing sand saturated with gasoline (GC) (Figure 5) in a sand-filled test pit (Loughridge, 1998). Gasoline has electric properties similar to

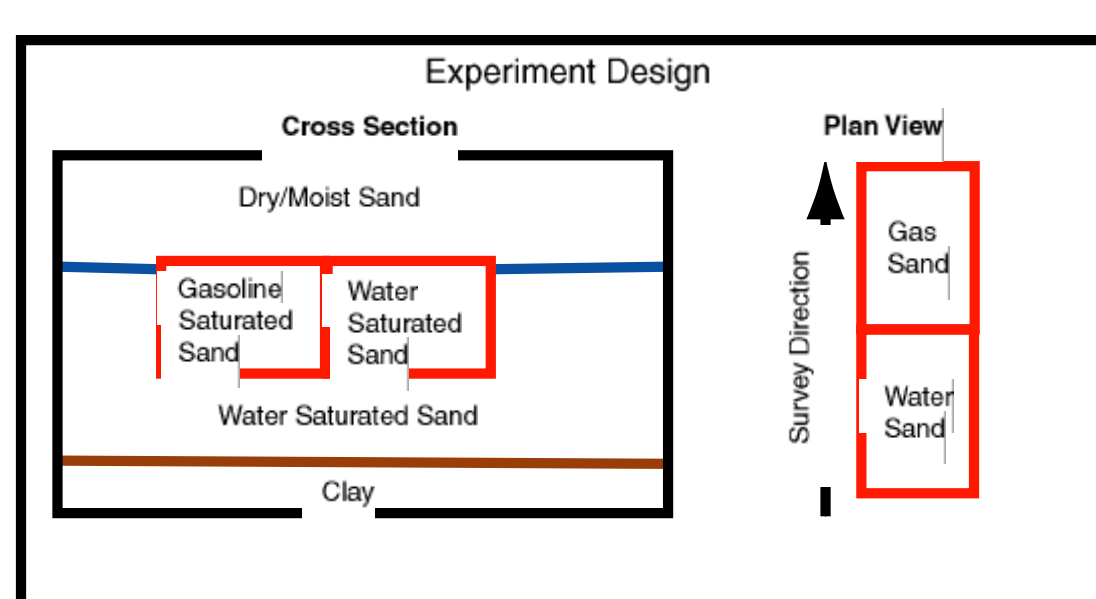


Figure 5: Schematic of the LNAPL AVO experiment. The containers are 46 cm x 30 cm x 41 cm and buried at a depth of 0.53 m.

## Principles of DNAPL Detection with GPR

The relative dielectric permittivity (K) and electric conductivity depend strongly on material type. The amplitude of a GPR reflection is dependent on the contrast of permittivity and conductivity at material boundaries, and attenuation of the signal is dependent on the conductivity of the material through which the signal is propagating (Davis and Annan, 1989). Water has very high relative permittivity (K=80), whereas common DNAPLs such as chlorinated solvents have very low relative permittivity (K=2) and are very poor conductors. Most dry earth materials, through which the GPR signal will propagate efficiently, have relatively low permittivity (K = 4 - 16) so that introduction of water into the pore space results in a significant increase in bulk permittivity of the three phase system (air, water, earth material). Thus, two types of sediment with different porosity that have similar permittivity when dry, can have significantly different permittivity when water is present in the pore space due to variations in bulk water concentration (Olhoeft, 1986). Additionally, the presence of water can significantly increase bulk conductivity, particularly in the presence of clay.

Anomalous displacement of naturally occurring water with low permittivity DNAPL leads to lower bulk permittivity and conductivity than the surrounding sediments. The amount of the contrast depends on the wetting phase and relative concentrations of water and DNAPL. Several modeling and laboratory studies have illustrated that when the organic is the wetting phase, the conductivity and dielectric permittivity drop sharply with very low concentrations of DNAPL, whereas the change is more gradual when water is the wetting phase (Endres and Redman, 1996; Santamarina and Fam, 1997). In a cross-well ERT field study, Newmark et al. (1998) recorded significant decreases in conductivity associated with pooled and residual TCE in water wet sediments at Hill, AFB, Utah. We expect a significant decrease in dielectric permittivity to correlate with the decrease in conductivity. The results of this study indicate that DNAPL detection potential using GPR can be very high in a field setting.

We expect the GPR signature associated with the presence of DNAPL to be manifest in essentially three ways. First, the decrease in dielectric permittivity results in increased EM propagation velocity. Secondly, the decrease in permittivity can significantly change reflectivity. If the NAPL is in a discrete pool or plume, we expect increased reflectivity or variations in the AVO response associated with the NAPL boundaries. If the NAPL is smeared vertically or has diffuse boundaries, as is the case for residual saturation, we may observe decreased reflectivity in the sediment column due to homogenization of the permittivity profile. This occurs because decreased bulk water content reduces porosity dependence (Olhoeft, 1986). Finally, the decrease in conductivity leads to decreased levels of signal attenuation.

chlorinated solvents and therefore the GPR attribute signature is similar. The containers (46 cm x 30 cm x 41 cm) were buried at a depth of .53 m, with the long axis oriented parallel to the survey direction (Figure 5). The pit sand is a coarse grained, washed quartz sand, and the same sand was used to fill the containers. The water table in the pit was maintained at a depth of .61 m, which is about 8 cm below the top of the containers.

Two, 2-D, CMP surveys, were acquired with a Senso and Software Pulse\_Ekko 1000 system using 450 MHz antennas. The data were acquired in expanding-spread CMP gathers. The first survey was acquired with parallel polarization antenna configuration and 30 traces/CMP (Figure 6). The second survey was acquired with transverse polarization antenna configuration and 32 traces/CMP (Figure 7).

We expect an anomalously large AVO gradient to be associated with the reflection from the top of GC. For first pass analysis, we use a seismic AVO attribute analysis routine to extract the AVO gradient from the parallel polarized dataset at all points in the profile. There are strong reflections associated with both the water and gasoline saturated sand, but only the gasoline sand reflection is associated with a large AVO gradient (Figure 8). The attribute display is a vivid representation, and the LNAPL is easily identified. We estimate the permittivity ratio at the reflector boundary, assuming that K (the dielectric constant) is approximately frequency independent. This assumption is reasonable for many GPR applications (Annan, 1998). When this assumption is valid, the value of Brewster's angle ( $\theta_B$ ) provides a precise estimate of  $\epsilon_1/\epsilon_2$ , where  $\epsilon_1$  and  $\epsilon_2$  are the dielectric constant for the lower and upper medium respectively (Griffiths, 1989). Considering the LNAPL reflection. Extracting the zero crossover angle  $\theta_B$  from CMPs 133 - 140, we find that  $\theta_B$  occurs at an angle of 36.9 degrees which corresponds to  $\epsilon_1/\epsilon_2 = 0.56$ . Migration velocity analysis and assumption of a linear velocity gradient above the target yields a value (at the boundary) of  $\epsilon_1/\epsilon_2 = (0.116 \text{ m/ns} / 0.162 \text{ m/ns})^2 = 0.51$ . The two results differ by only 8.4%, and the good correlation serves to support both the velocity and  $\epsilon$  analyses.

Using a physical model, we have demonstrated significant potential to use the GPR AVO response as a NAPL indicator. The gradient attribute can be used as an easy to interpret reconnaissance tool, and  $\epsilon$  can be used to extract precise values of  $\epsilon_1/\epsilon_2$ . The AVO attribute extraction algorithms need to be optimized for GPR studies. Most importantly, continued experiments are needed to determine how well the technique works under field conditions where the contaminant boundaries are more diffuse.

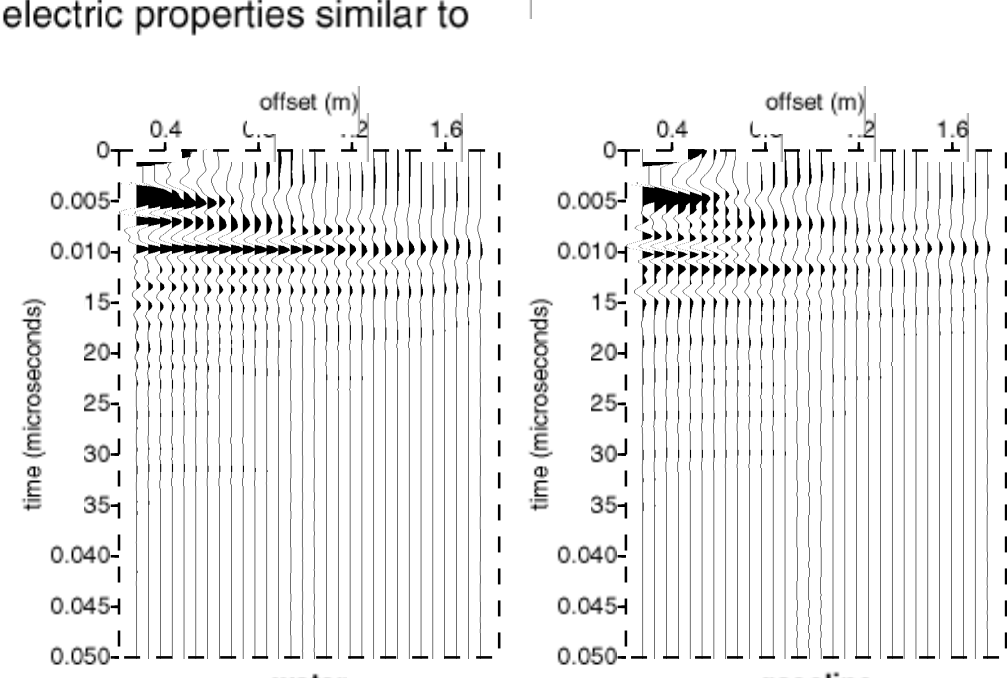


Figure 6: Representative data from the GPR physical model. Shown are NMO corrected CMP gathers, acquired in parallel polarized antenna configuration. The water and NAPL reflections are at a time of about 0.09 microseconds. Note the occurrence of Brewster's angle for the gasoline reflection at an offset of about 1 m.

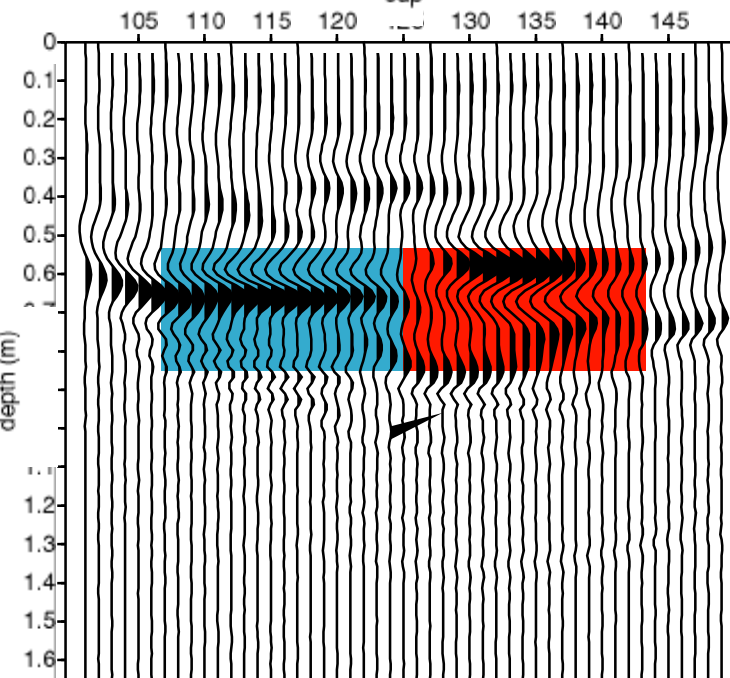


Figure 7: Pre-stack depth migrated image of the containers with gasoline (red) and water (blue) saturated sand. Colored regions indicate actual positions and dimensions of the containers. These data were acquired in transverse polarization mode.

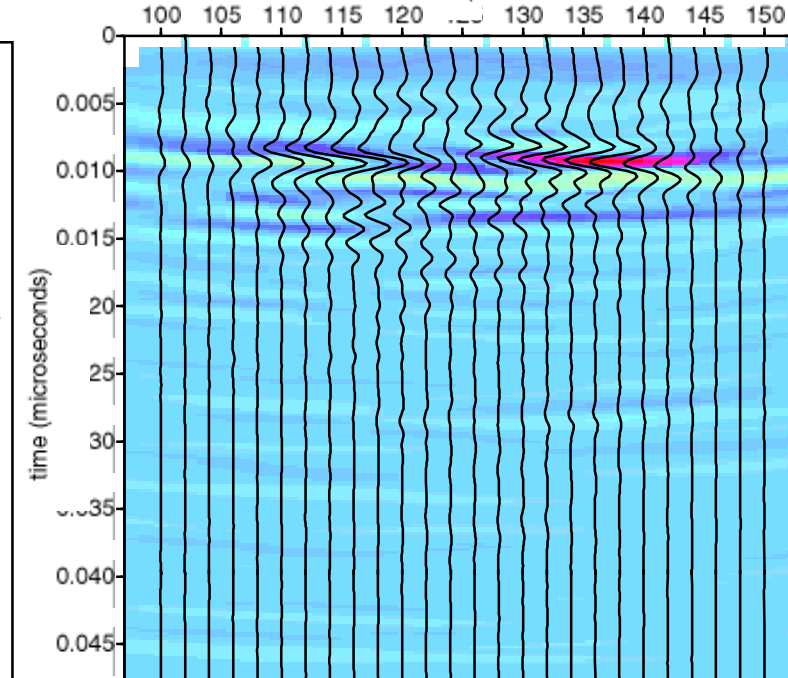


Figure 8: AVO attribute image and pre-stack time migrated wiggle trace overlay. The attribute was calculated from the parallel polarized data, the overlay is the transverse data. Red indicates a large AVO gradient associated with the top-of-NAPL reflection.

A number of previous workers have investigated the potential to detect both DNAPL and LNAPL using GPR (Annan et al., 1992; Campbell et al., 1995; Daniels et al., 1995; DeRyck et al., 1993; Powers and Olhoeft, 1996; Saunders et al., 1993). Grumman and Daniels (1995) review a number of organic contaminant studies for both vadose and saturated zone applications. In general the published studies have met with moderate or variable success, but so far have relied on relatively simplistic data processing schemes and qualitative interpretation of GPR signal anomalies. While this may be sufficient under tightly controlled conditions where the location of contaminants is known, these techniques are not adequate for exploratory studies or where the GPR NAPL response is more subtle. Our approach is to combine detailed velocity analysis and imaging with reflected waveform attribute analysis to produce detailed, quantitative subsurface images and material property maps that can be used to predict the location of subsurface contaminants. This approach will dramatically improve contaminant detection success rates and the reliability of the GPR method.

An important component of this project is the development of predictive forward modeling tools. Realistic modeling requires accurate modeling of both contaminant distribution and electromagnetic wave propagation. We have begun integrating three-phase flow and GPR response modeling in planning a controlled tetrachloroethylene (PCE) injection experiment which will be conducted at Dover AFB in June and July of 2000. The finite element, multi-phase flow code (NAPL Simulator), was authored by Guarnaccia et al., 1997, and is available from EPA's Center for Subsurface Modeling Support. Fluid concentrations output by the flow model are used to generate a dielectric permittivity model using a time average equation. The GPR response is then calculated using a 2-D, acoustic, finite difference scheme. The acoustic code is appropriate for modeling transverse polarized wavefield kinematics and amplitudes assuming a 2-D earth and zero conductivity. One objective of the project is to develop a wave-equation based GPR modeling code which correctly accounts for transverse and parallel polarized fields, and frequency dependent material properties.

For the Dover AFB experiment, PCE will be injected into an isolated test cell that was constructed by driving steel sheet piling into a natural aquifer. The experiment will be highly controlled, this will provide an excellent opportunity to test both our predictive modeling capabilities, and for field testing various GPR contaminant indicators. The site is only permitted to release 100 l of PCE for any given experiment, and it is important we determine if this volume of contaminant will produce a significant GPR response. Figure 2 illustrates the time varying flow model and GPR response for a 50 l injection. The GPR data are modeled using a 100 MHz source wavelet, and show a clear response to the DNAPL injection. There is a clear reflection from the NAPL pool itself, and there is a significant increase in velocity as evidenced by the pull-up of the no-flow boundary reflection. Based on these results, we conclude that a 100 l injection will be adequate to meet our experiment objectives.

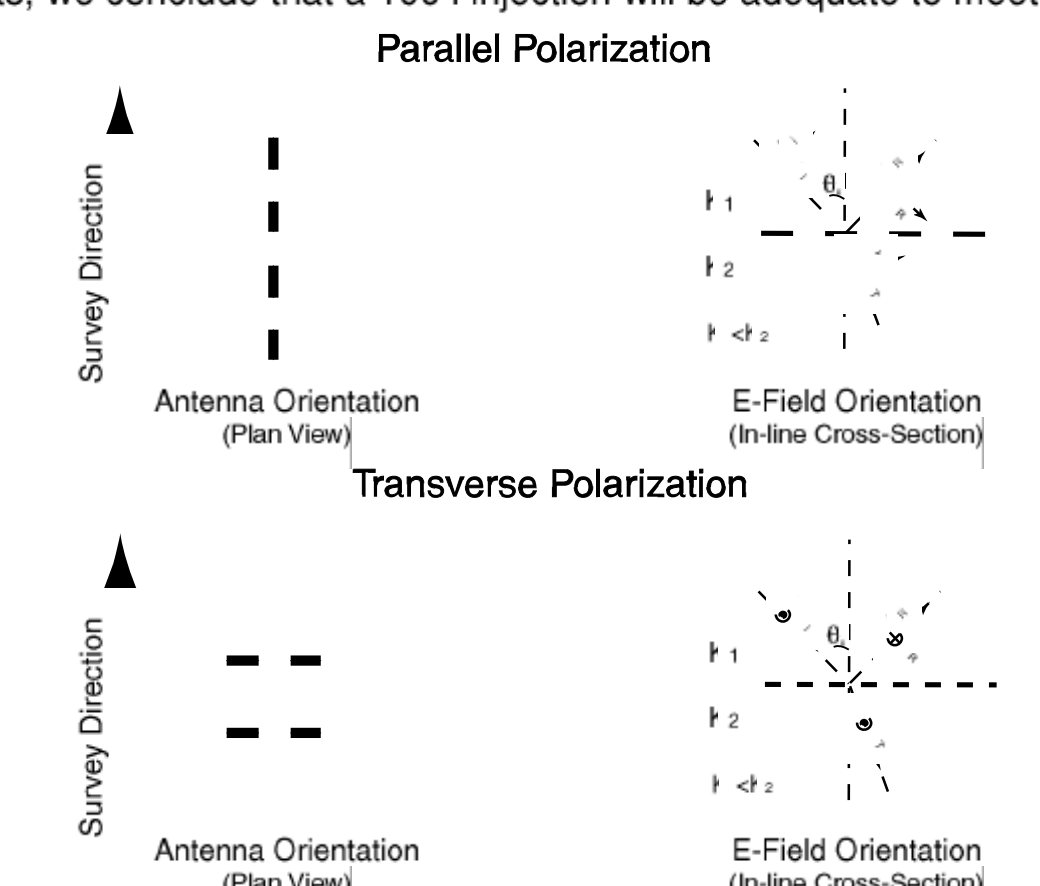


Figure 3: Antenna and electric field orientations for parallel and transverse polarization configurations. k and E are the unit vectors for the wavenumber and electric field respectively.

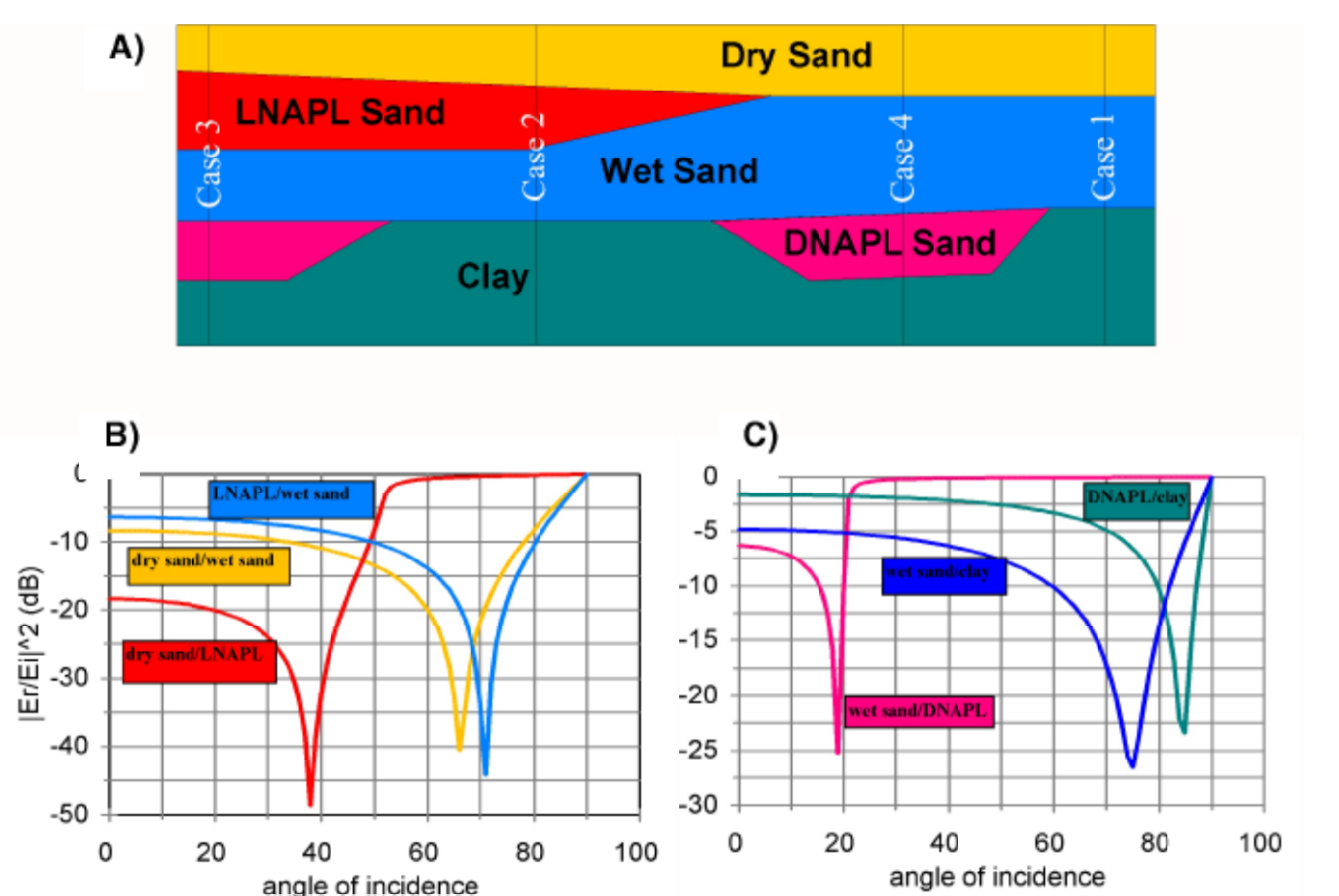
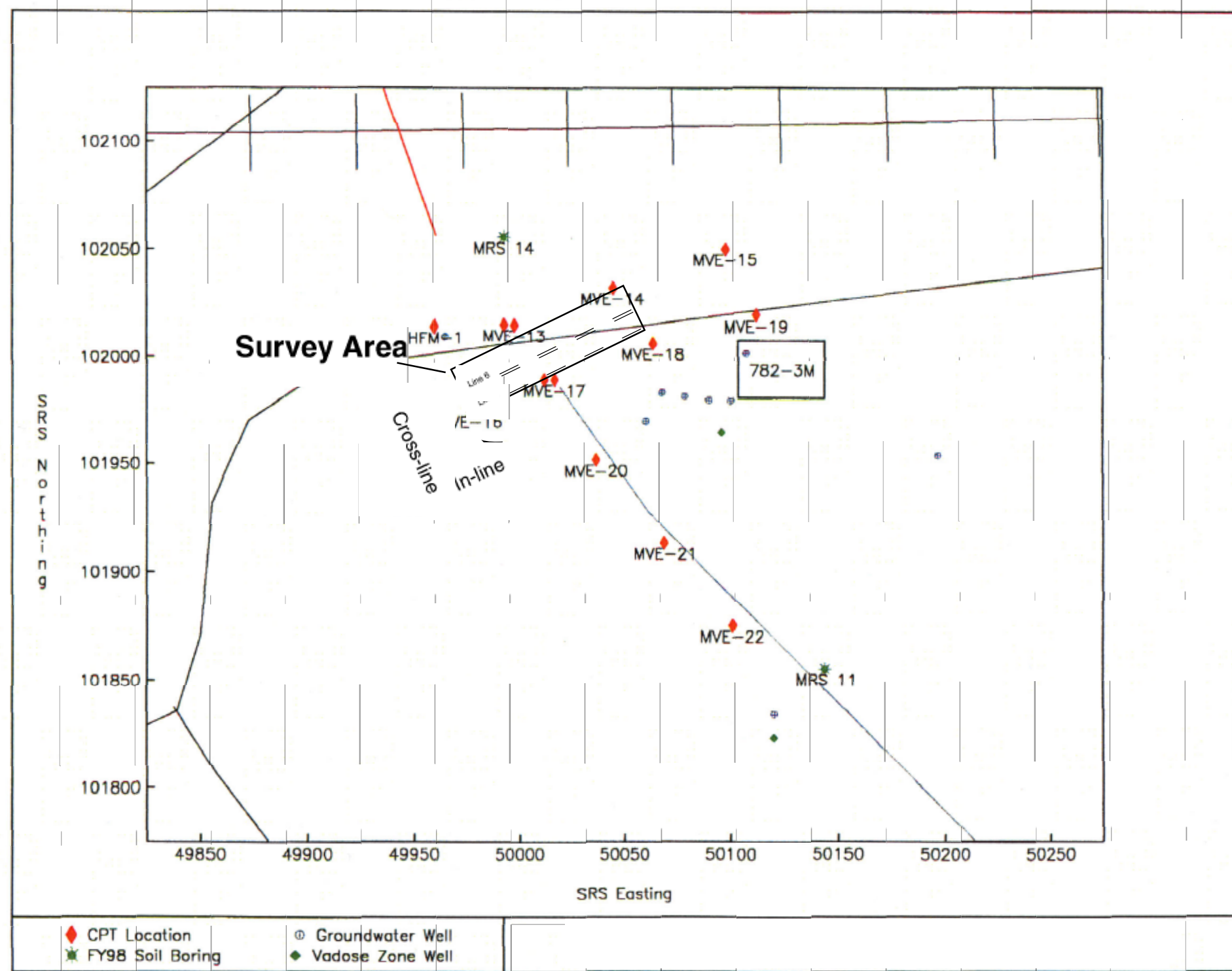


Figure 4: Reflection coefficients vs. angle of incidence for the possible reflecting interfaces in a hypothetical aquifer contaminated with both LNAPLs and DNAPLs. B) Note the dramatic difference in AVO response for a reflection from the top of the LNAPL sand (dry sand/LNAPL sand) as a reflection from the water saturated zone (dry sand/wet sand). C) The effect is even more pronounced for a reflection from the DNAPL sand (wet sand/ DNAPL sand) vs a reflection from the clay (wet sand/clay). At Brewster's angle, the reflection amplitude goes to zero. We find that Brewster's angle occurs at much smaller angles of incidence for the top-of-NAPL reflections than for the other possible reflecting interfaces in the model.

# Savannah River Field Study



**Figure 9:** Study location at the Savannah River Site. Survey area box shows location of full-fold, 3-D patch. Previous workers discovered DNAPL at depths less than 20 ft at CPT locations MVE-13 and MVE-17 which are indicated with blue red diamonds (Jackson, et al, 1999). Shallow depths, known location of significant DNAPL accumulation, and the ability to span the contaminated zone in a relatively short distance make this an excellent location for a GPR NAPL detection experiment. (Modified from Jackson et al, 1999)

## Site Background and Description of Field Work

Between 1952 and 1979, approximately 1,395,000 lbs of chlorinated solvents were released at the A-014 outfall of A/M area (U) at the Savannah River site (Jackson et al, 1999). About 72% was tetrachloroethylene (PCE). Until recently, it was thought that significant concentrations of DNAPL were confined to the deeper section of the vadose zone. In 1999, significant accumulations of solvent were discovered at depths less than 30 ft in the vicinity of the A-014 outfall (Figure 9).

Sediments at the site consist of relatively coarse grained sands at the surface, a primarily kaolinitic clay layer at a depth ranging from 5 - 10 ft, and a thick, coarse grained sand unit at with top-of-sand at a depth of about 22 ft.

In January, 2000, we conducted a 2366 sq. ft., 3-D, multi-offset, GPR survey at the A-014 outfall (Figure 9). The survey was designed to encompass the shallow DNAPL zone, with little or no contamination near the edges and a strongly contaminated zone near the center. Kaolinite typically has relatively low conductivity, so we felt there was a good chance we could penetrate the clay. Two severe winter storms in one week (highly unusual in the southeast) forced us to cover only about one quarter of the area designated in the original plan.

The 3-D patch is 26 ft in the cross-line direction and 91 ft in the in-line direction (Figure 9). Data were acquired with a Sensors and Software PulseEKKO 100 system with 100 MHz antennas. Thirteen transects were acquired in the in-line direction with a line spacing of 2 ft. Continuous multi-offset data were acquired every other line (Figure 10), so that the spacing between multi-offset lines is 4 ft. Multi-offset data were acquired with a 6 ft minimum offset, 2 ft shot interval, 1 ft receiver interval, and 30 traces per shot. Common-offset lines were shot with 6 ft minimum offset and 1 ft trace interval. All data presented here were acquired in parallel polarization antenna configuration.

The scaled back experiment has already produced some very interesting and promising results. Data analysis is ongoing and the results presented here, although promising, should be considered preliminary.



**Figure 10:** Multi-offset data acquisition at the Savannah River Site. Research Assistant Ryan Athey is shown manning the GPR antennas.

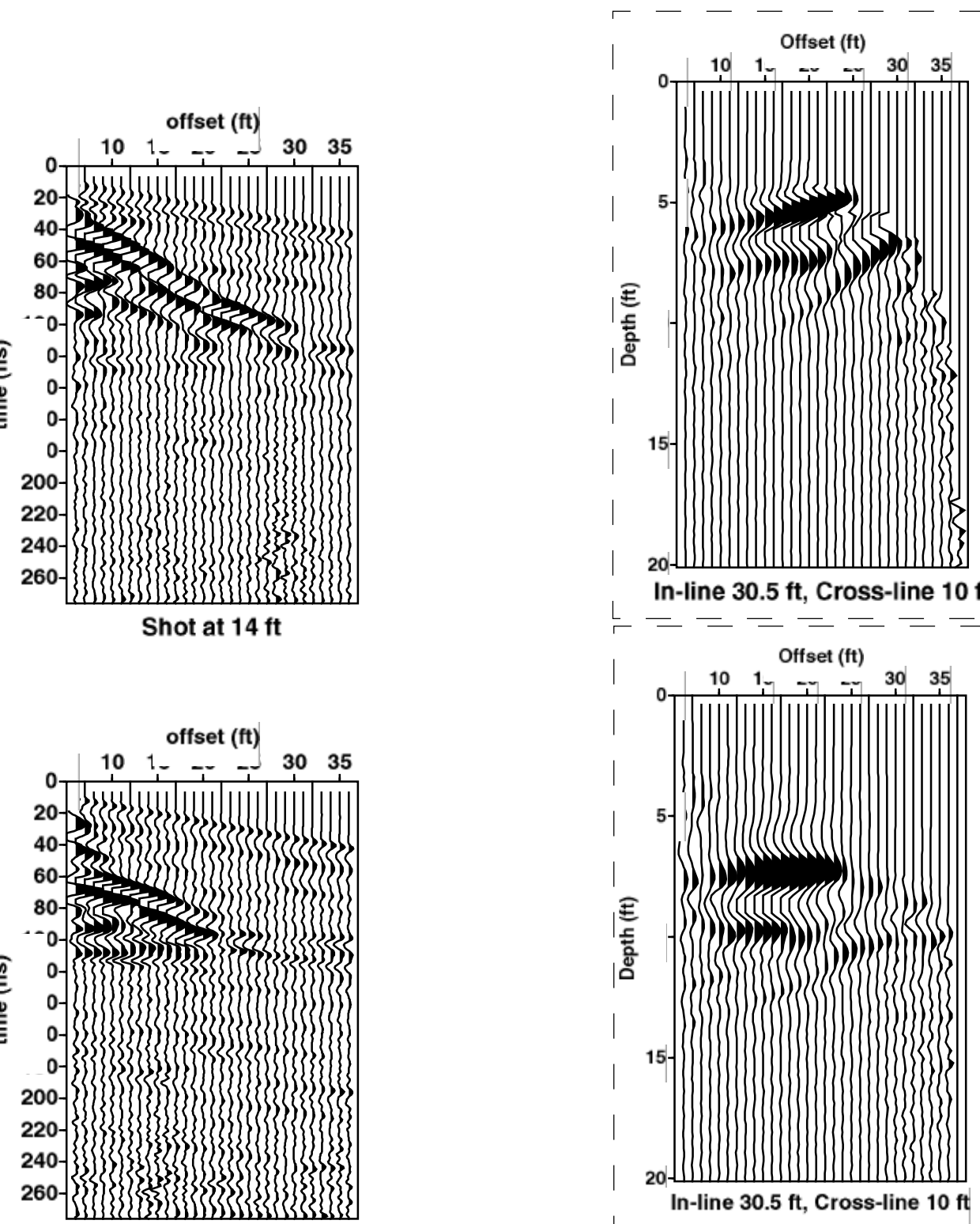


**Figure 11:** Representative shot gathers from Line 5. The direct wave in the shot at 14 ft shows a significant stop change at an offset of 21 ft indicating a sharp and significant increase in velocity. This lateral velocity heterogeneity calls for pre-stack migration velocity analysis. The reflection from the base of the channel shows up at about 60 ns in the shot at 28 ft.

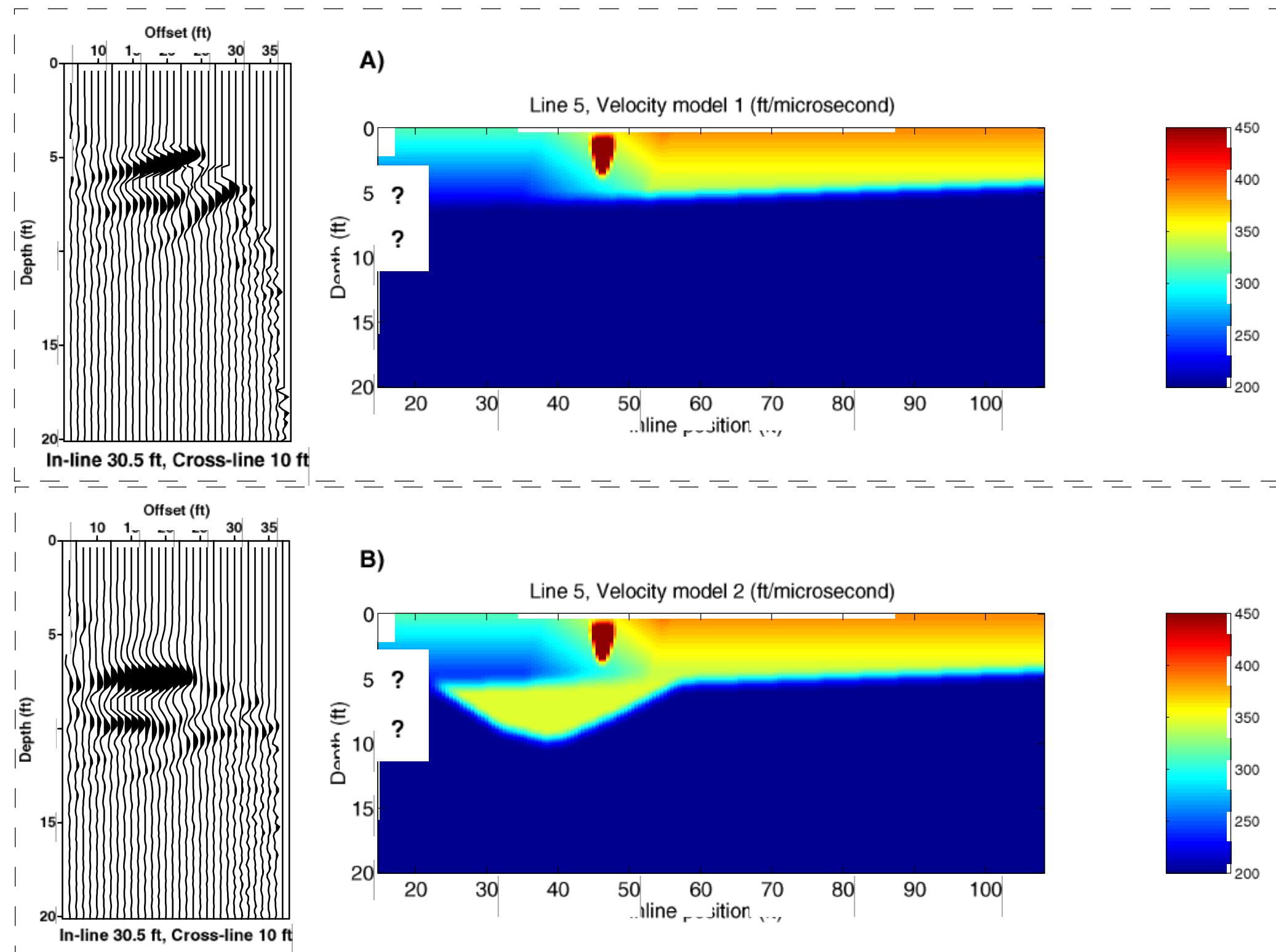


**Figure 12:** A preliminary velocity model A), and final velocity model B) with common-image point gathers illustrate the process of pre-stack depth migration velocity analysis. For velocity model 1, the surface velocity is measured from the direct wave and is very accurate. Velocity below 5 ft is assumed based on published values for kaolinite at 30% water saturation. The shallow velocity gradient is estimated based on the assumption of increasing water content with depth. The dark red spot is the void space associated with the outfall ditch and is 1000 ft/ns. Velocity model 1 works well for all data regions except within the shallow channel between 25 and 55 ft. Pre-stack depth migration with velocity model 1 does not flatten the base-of-channel reflection. Inserting a high velocity zone within the channel results in correct migration of the base-of-channel reflection (B). The lateral change in surface velocity is related to changes in water saturation which appears to be more strongly controlled by lithology than vicinity to the outfall (see Figure 15). The velocity model is incorrect between in-line positions 15 and 25 ft at depths between 5 and 10 ft. Further analysis is needed to understand the velocity structure in this region.

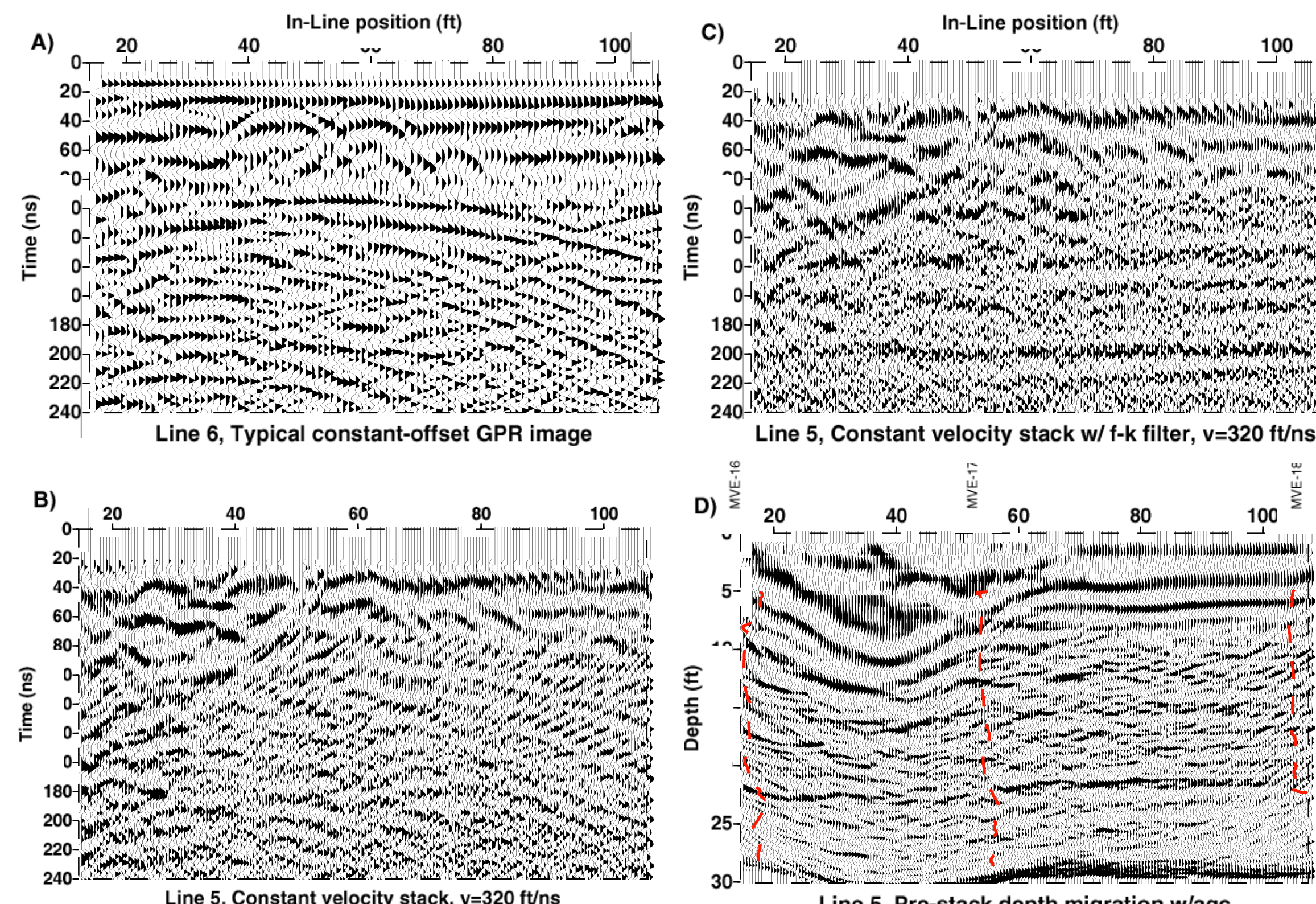


**Figure 13:** A) A typical GPR profile gives some indication of subsurface reflections, most notably the base of channel reflection at a time of 65 ns between 25 and 35 ft. The section is dominated by surface scatter below 90 ns. B) Stacking attenuates the surface scatter, but there are still no interpretable reflections below 90 ns. C) Applying an f-k filter to remove air velocity events (surface scatter), followed by stacking results in dramatic reduction in surface scatter noise. A subsurface reflection at about 200 ns is now evident. D) Pre-stack depth migration is strongly dependent on velocity and serves to further attenuate surface scatter. Resistivity logs from CPT locations MVE-16, MVE-17, and MVE-18 show a sharp increase at a depth of about 22 ft which corresponds to the boundary between the clay and the underlying sands. This shows excellent correlation with the depth migrated image. The shape of the sand-clay interface at 4-9 ft is nicely imaged and clearly shows the channel, although moisture content data indicate that the reflection is actually originating from an increase in water saturation slightly above the clay boundary (see Figure 14). A flat event is evident from an in-line position of 50 ft to 70 ft at a depth of about 11 ft. This correlates with the shallowest depth at which DNAPL was found in MVE 13 and MVE 17, and is fairly consistent across all the lines. It may be a lateral DNAPL migration route from the base of the channel, but is a very weak event and is overwhelmed by noise in the pre-processed gathers, therefore we cannot make a confident interpretation at this time.

## Multi-offset Data Acquisition and Velocity Estimation

Most GPR surveys are acquired with a constant transmitter-receiver offset (bi-static mode) and little or no processing is employed in generating the final image. This can provide useful information and is valuable as a rapid reconnaissance tool. However, as the complexity of the EM velocity structure increases, and/or the signal-to-noise ratio decreases, the ability to produce useful images using this simple acquisition geometry diminishes. EV velocity estimates cannot be made from common-offset data, therefore reflector depth estimates must be based on rough guesses of material velocity or correlation of interpreted reflectors with known material boundaries. This is highly unreliable if there is significant lateral velocity heterogeneity.

In multi-offset data acquisition, several traces are recorded at various source-receiver separations at each point along the survey, as opposed to a single trace at each point for a constant-offset survey. This is the standard acquisition procedure in reflection seismology, but is not often used in GPR studies, which is, at least in part, due to equipment limitations. Multi-offset acquisition, while more labor intensive and time consuming, significantly improves our ability to accurately predict the subsurface. At the Savannah River site, multi-offset data is proving extremely valuable in our understanding of the subsurface for two primary reasons:

1) Multi-offset data provide traveltimes vs. offset curves, which enable one to estimate propagation velocity. Velocity analysis is necessary for estimating depth and provides a direct estimate of electric permittivity. When there is little velocity heterogeneity, and the gradients are small, velocity can be estimated using standard normal-moveout velocity analysis. But when there are large vertical or lateral velocity gradients, as is the case at the Savannah River site, a more accurate tool is needed for both velocity analysis and imaging. We use pre-stack depth migration velocity analysis, which provides the most accurate velocity model and detailed images of any current technology (Figures 11 and 12).

2) Dramatic attenuation of coherent noise is achieved through velocity filtering and random and coherent noise are further attenuated through stacking. In this case, we are applying a velocity filter in the frequency-wavenumber (f-k) domain to remove surface scatter since the waves traveling through air are traveling at a much higher velocity than those traveling in the subsurface. To produce a stacked image, all reflected events are flattened, either by applying a normal moveout correction, or by pre-stack migration. Traces in common-midpoint (or common-image point for migration) are then summed to produce a single stacked trace at each CMP location. Coherent or flattened reflections stack constructively, while noise events are attenuated. Since this is a velocity dependent process stacking also acts as an effective velocity filter (Figure 13).

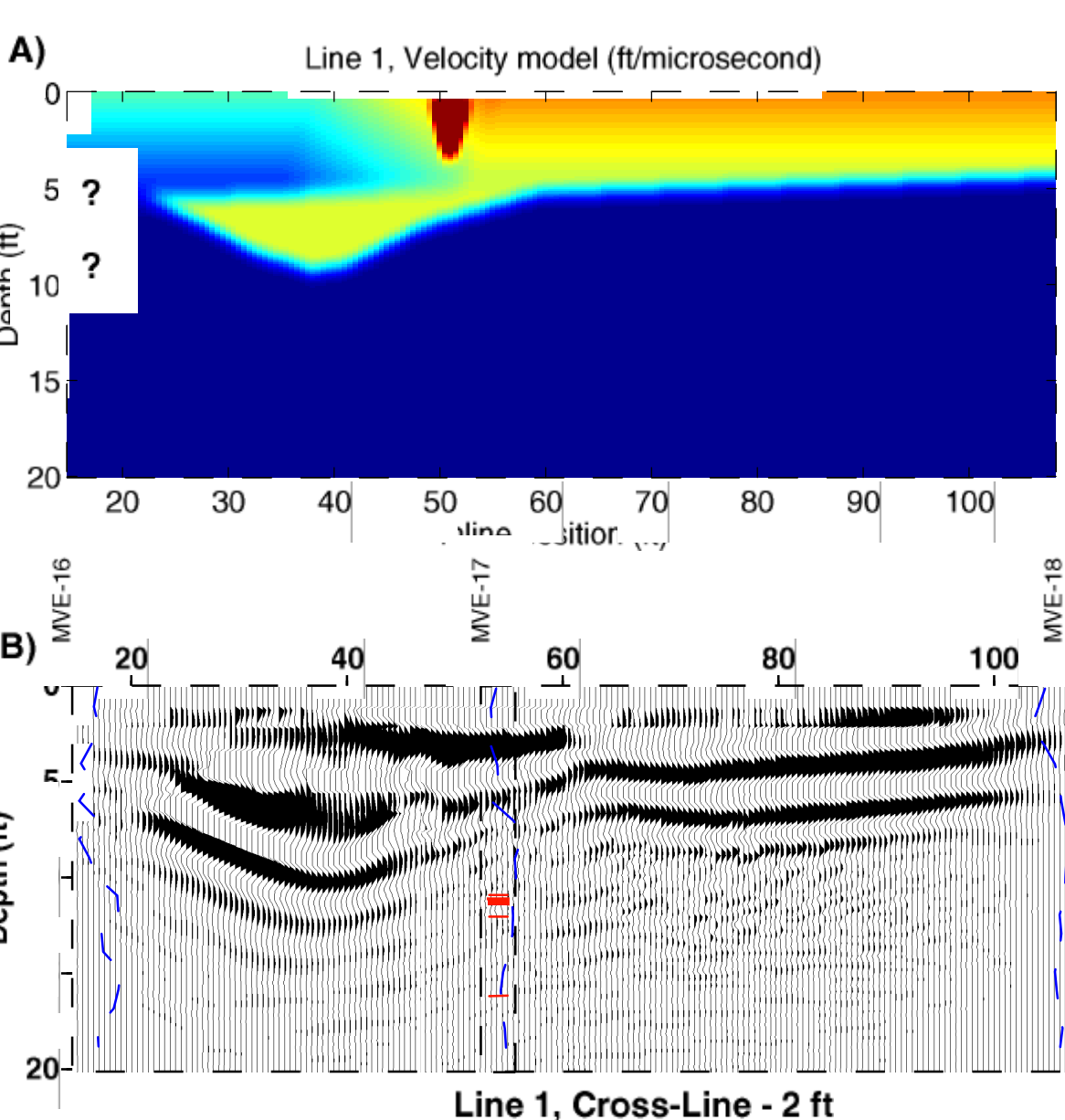


**Figure 14:** A) Migration velocity model for Line 1. B) Pre-stack depth migrated image. Neutron logs converted to water saturation from MVE-16, MVE-17, and MVE-18 are overlain. Also a log showing the position of observed DNAPL in MVE-17 is shown with the presence of DNAPL indicated in red. The continuous reflection from in-line positions 25 to 106 ft appears to correlate with an increase in moisture content that is slightly shallower than the top-of-clay surface. This is expected and the reflector likely tracks the top-of-clay topography. The velocity model at MVE-16 is not correct, and any attempt to correlate shallow reflections with the moisture log in this location is not appropriate. A flat event below MVE-17 appears to correlate with the top-of-DNAPL, and is consistent across several lines (see Figure 13). However, the quality of data in this zone does not warrant a confident interpretation at this time. Further processing and analysis is necessary. The topographic low between in-line positions 25 and 55 ft is interpreted as a channel and is consistent across the entire survey. This feature has not been previously identified. C) Contour map of the shallow, continuous reflection showing the shape and orientation of the channel. The current position of the A-014 outfall ditch is shown with a dashed line. The position of the channel does not correlate with the orientation of the outfall ditch so we can be confident that the event is not a data artifact related to the large velocity anomaly associated with the outfall ditch. It seems likely that the channel acted as a DNAPL migration route, and that high concentrations of DNAPL remain in the channel fill, particularly given the presence of significant DNAPL accumulations in the clay below MVE-17.

## Preliminary Results and Discussion

To date, we have completed a preliminary 3-D velocity model and initial interpretations of the data correlate reasonably well with available lithologic, electric resistivity, and water content data (Figures 13-15). Further refinement of the velocity model is necessary, and once this is completed we will begin more detailed attribute analysis.

Using pre-stack depth migration velocity analysis and imaging, we have identified a high velocity anomaly associated with a channel-like feature that had not been previously identified. The channel appears to cut about 3-4 ft into the top of the clay, is adjacent to known areas of DNAPL concentration and lies below the current position of the A-14 outfall (Figure 14). Since the channel is directly below the outfall, which maintains a stream of running water, we would expect higher water saturation, and therefore lower velocities within the channel. However, the velocity within the channel (350 ft/ns) is near the highest velocity in the survey (390 ft/ns) which is measured from the direct wave traveling at the surface near the east side of the survey. Our initial interpretation is that this channel formed a DNAPL migration route, and that once trapped at the base of the channel, DNAPL migrated laterally into the adjacent clay formation where it is currently observed. The high velocity within the trough may be related to either pooled DNAPL or high levels of residual DNAPL concentration. We are currently planning to acquire additional soil samples within the channel to verify this interpretation.

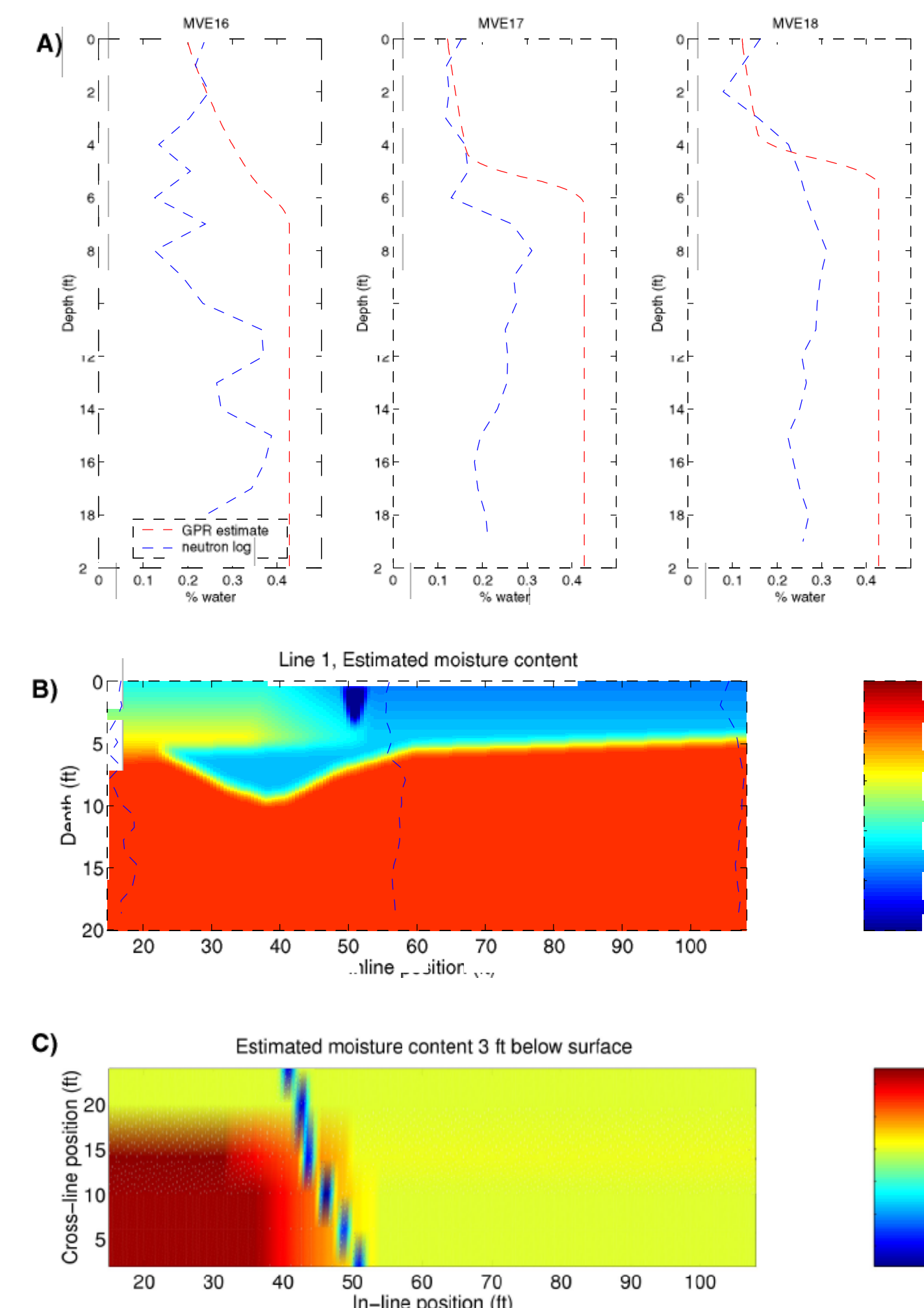


**Figure 15:** A) Water saturation from neutron logs, and estimated from GPR velocity data. The GPR estimate at MVE-15 is only valid within about 3 ft of the surface. Water content is estimated from GPR data using a time average equation given by:  $S_w = (t^{1/2} - (1-p) \cdot t^{1/2} - p) / (t^{1/2} - 1)$  where  $p$  is porosity,  $\epsilon_s$  is the dielectric constant of the soil grains, and  $\epsilon_w$  is the dielectric constant of water. In this case, we assume  $p=0.4$ ,  $\epsilon_s = 4.5$ , and  $\epsilon_w = 80$ . This equation works well for sandy sediments with very low conductivity. The GPR estimates correlate very well with the neutron logs near the surface. The correlation is not as good in the clay where the time average equation is less accurate. B) Water saturation estimates along Line 1 with neutron logs overlain. Assuming no DNAPL is present,  $S_w$  in the channel is less than 15% which seems unlikely given the proximity to the outfall ditch particularly if there is no impediment to flow between 3 and 10 ft. The presence of a DNAPL pool could account for the low apparent water content. C) Depth slice of the  $S_w$  estimate at 3 ft. There is a significant increase in water content in the vicinity of MVE-16 which does not correlate with the outfall ditch. This suggests that the change is related to lithology, although we don't presently have the data to confirm this interpretation.